applied sciences

MDPI

Article

Measurement Repeatability of Rail Wheel Loads Caused by Rolling Surface Damages

Gediminas Vaičiūnas *, Gintautas Bureika and Stasys Steišūnas

Faculty of Transport Engineering, Vilnius Gediminas Technical University (VILNIUS TECH), Plytinės Str. 25, 10105 Vilnius, Lithuania

* Correspondence: gediminas.vaiciunas@vilniustech.lt; Tel.: +37-0610-15376

Abstract: The repeatability of rail wheel damage measurements is considered in this study. The authors investigated the measurement repeatability of vertical force dependence on wheel-rolling surface damage nature and suggested ways to reach higher repeatability. To investigate wheel-rolling surface damage impact on vertical force measurement repeatability, the results of measuring forces with different measurement systems were compared first. Another critical issue was estimating the deviation field for the measured force values. The box and whisker principles were used. Different types (shapes) of rail wheel damages and rolling stock operating conditions were examined by field tests. The article presents the dependence determined by the authors, and how the repeatability of the wheel damage measurement depends on the speed of the rolling stock.

Keywords: rail transport; wheel-rolling surface; wheel vertical loads; wheel flat; measurement repeatability; box and whisker methods

Citation: Vaičiūnas, G.; Bureika, G.; Steišūnas, S. Measurement Repeatability of Rail Wheel Loads Caused by Rolling Surface Damages. *Appl. Sci.* **2023**, *13*, 4474. https://doi.org/10.3390/app13074474

Academic Editor: Diogo Ribeiro

Received: 16 February 2023
Revised: 9 March 2023
Accepted: 15 March 2023
Published: 31 March 2023

1. Introduction

Track failures or rail vehicle derailments represent approximately 50% of overall accidents in railway transport [1]. The majority of the track integrity problems are related to the track geometry or gauge distortion. Other factors that harmfully impact on properness of wheel–rail contact are badly repaired running gear, discrepancy of rails, and critical dynamical impacts (such as high tractive and braking forces of trains). Furthermore, some railway traffic accidents happen due to the diminishing of reliable wheel/rail contact and due to the unsatisfactory stability of rolling-stock running. [2].

The parameters and shape of the rolling surface of the rail wheel mainly influence the technical condition of rolling stock running gear. The "wheel-rail" contact transfers high vertical static and dynamic loads to the vehicle and the track [3]. As the wheel rolls, high-impact loads are created by track irregularities and rail junctions [4]. During rolling-stock exploitation, the interaction between the wheel and the rail may cause damage to the rolling surface of the rail wheel [5]. They can also be caused by manufacturing inaccuracies [6] or poor machining [7]. It should be noted that the occurrence of damage is most affected by braking and track surface irregularities [8]. The damage of the wheel rolling surface is very destructive to the upper track structure. It can also cause wheel cracks and derailment of the wagons [9]. Polish scientists Burdzik et al. defined the dynamical properties of the driving train and evaluated the technical state of the rail track by using proprietary measurement software and a mobile device. Authors proposed useful metrics to describe the dynamical properties of the driving train [10]. Strikes of damaged wheels produce high noise and vibrations that impair passengers' comfort [11]. Vertical interactions of the wheel with the rail acquire an impact character when the wheel is damaged. These studies require unique methods since the processes under investigation have a higher frequency [12]. Polish scientists Celinski et al. defined the dynamical properties of the driving train and the evaluated the technical state of the rail

track by using proprietary measurement software and a mobile device [13]. Furthermore, authors proposed useful metrics to describe the dynamical properties of the driving train. R. Burdzik et al. considered the impact of rail damage on vibration waveforms and vibroacoustic spectrum images of vibrations. The major source of railway vibration is the structural vibration of the wheel and rail, which is generated by the combination of small-scale undulations on the wheel and rail contact surfaces. The inevitable vibration transmitted by running rail vehicles through the rails and wheels causes and propagates various cracks in the metal of running gear elements. The authors revealed the amplification of the signal from the Ai3 sensor located near the damaged place where the frequency oscillated around 4000 Hz, while the spectral analysis of the signal for the Ai2 sensor located 5.4 m away to the damage indicated oscillating values in the range from 50 to 500 Hz [14]. Depending on the train's speed, the maximum duration of the force is in the order of several milliseconds. The ATLAS-LG subsystem of wayside equipment is used by Lithuanian Railways (LTG) to detect and prevent damage due to their impact. ATLAS-LG type systems are used by Lithuanian and Swiss Railways and are designed to avoid traffic accidents. These systems detect passing wagon running gear that causes vertical impact loads on the rail track, which can be caused by damage to the wheel rolling surface (e.g., flat, crack, uneven wear, and "out-of-roundness").

Worldwide rigorous research activities are targeting not only security. A high level of safety and reliability of infrastructure systems also aims to diminish the problems associated with the degradation of performance in terms of train-ride quality and stability, passenger comfort, etc. To ensure the railway transport safety, decision-makers of rail companies need, inevitably, to monitor the geometrical parameters of the track and the condition of the vehicle wheel rolling surfaces. Wheel damage (flats, crumbling, cavities, cracks, wear, out-of-roundness, etc.) endangers traffic safety, i.e., the risk of derailment. The intensive damaging of the rails and track as a whole track geometry also increases.

Mathematical models of the impact of wheel flat damage on the rail usually developed using the reverse Laplace transformation methodology. These models were later developed by researchers from Ukraine and other countries [15]. It is noted in the literature that it is not entirely clear how short-term loads affect the systemic wear of the wheel surface. It is preliminarily known that the wear processes are influenced by such factors as surface irregularities and roughness, material hardness, and elasticity [11]. Due to the large number of factors, processes are modeled by simplifying them [16]. As an example, one can give the fact that elastic and plastic deformations and the formation of metal cracks as a result of them are not always taken into account when modelling processes [17]. In order to create a more reliable wheel wear prediction tree, it is necessary to evaluate not only one or two factors, but many more, perhaps a dozen or a few tens [18].

Both when examining wheel damage and when examining the causes of traffic accidents, it can be seen that wheel damage frequently causes traffic accidents (on the railway, traffic accidents are considered not only accidents with drastic consequences, but also minor incidents when train traffic is stopped for a short time) [19]. Flats and cracks are the most common damage of the rolling surface of the wheel to rail [20]. As rolling stock speeds increase, increasing dynamic forces affect the development of damages [21]. According to the impact on traffic safety, it is accepted to preliminarily divide wheel-rolling surface damage into two types [22]:

1. Damages that cause a short-term loss of wheel–rail adhesion (cracks, flats, bends);
2. Damages that do not cause loss of wheel–rail adhesion (e.g., uneven wear).

Some of the wheel damage may go unnoticed during the external inspection due to the human factor, so it is necessary to improve the automatic damage detection systems [23]. Different diagnostic systems associate the magnitude of the wheel surface damage differently with the impact force (the data processing algorithms used for this purpose may differ).

This study aimed to determine whether the repeatability of force measurement is more determined by the nature of the wheel damage or the driving speed, and to determine whether it is possible to detect the laws of the dependence of the repeatability of this measurement on the cause.

2. Analysis of Rolling-Stock Wheel-Rolling Surface Damage

During rolling stock inspections at railway stations, wheel damage is detected by templates and other devices (Figure 1). An external inspection identifies visible damages, such as wheel flats or cracks, and templates are used to inspect the wheel profile. Ultrasonic and magnetic defectoscopes are used to detect cracks in the wheel.

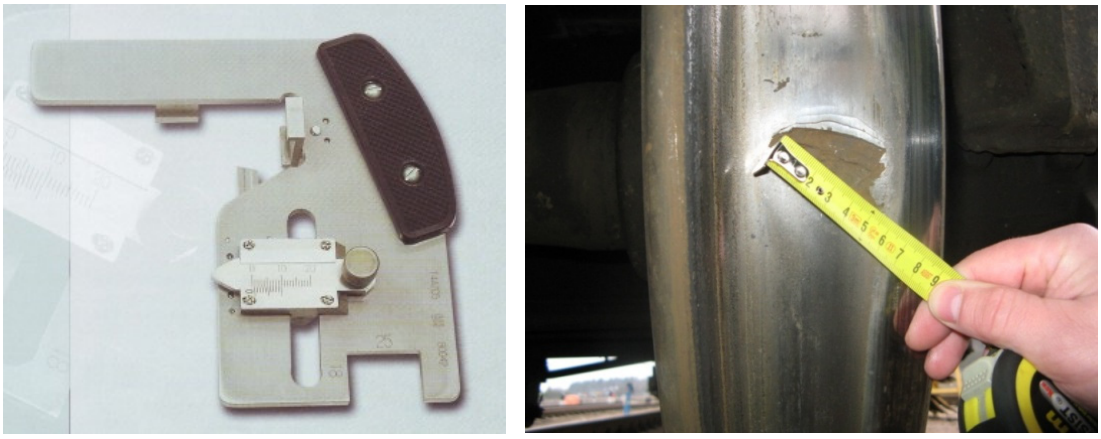

Figure 1. Wheel measurement template and measurement with a ruler.

The main damages of the rail wheels are the wear of the rolling surface, thinning of the flange, flats, cracks, and metal folds of the surface. The main types (shapes) of wheel-rolling surface damages are shown in Figure 2.

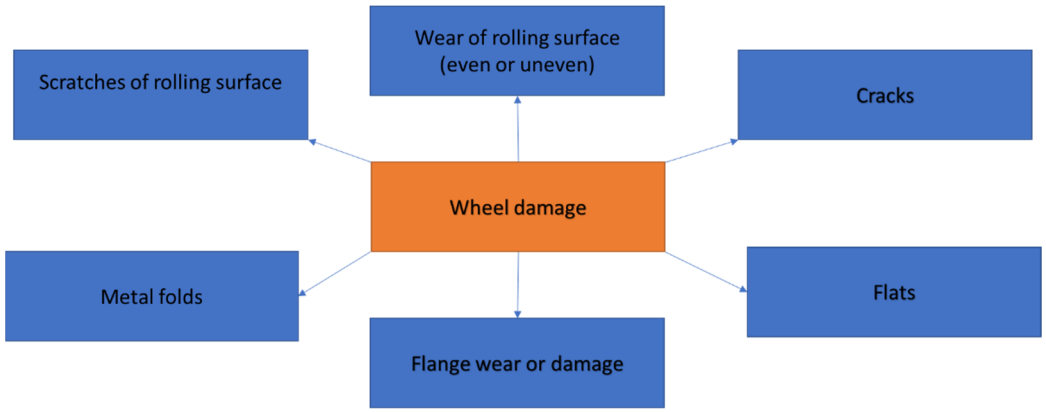

Figure 2. Main nature of damage of wheel rolling surface.

Flange damage. The wheel flange prevents the wheel from derailing. A wheel is considered damaged when its flange is critically thinned (up to 25 mm).

Metal folds. Metal folds occur in the presence of thermomechanical damage [24]. Intense plastic deformation of the metal occurs due to sudden braking, short-term wheel slip, wheel jumping, or sudden heating of the wheel metal, and then sudden cooling [25]. Several metal folds can be formed on the rolling surface of the wheel, as well as being in one or several layers. When the wheel of a passenger car has a metal fold up to 0.5 mm, or a freight wagon up to 1 mm, operation of the wagon is prohibited.

Rolling surface wear. Most publications on the long-term interaction between rolling stock and track deal with the wear of rail and wheel [26–28]. The phenomenon of wheel

wear has been extensively studied [29]. With the wear of the rolling surface of the wheel, train resistance to movement and the wheel/rail adhesion increase [30]. The wear of the rolling surface of the wheel is divided into even and uneven.

Uneven wear. This wear is special in that it does not have a dimensional extremity (such as the deepest point), so sometimes this type of wear is difficult to detect by the values of the dynamic diagnostic indicators [31]. The consequence of such wear is isolated wheel irregularities [32].

Flats. These are the most common wheel damage caused by wheel slip or a brake pad stuck [33], as shown in Figure 3.

Figure 3. Sample of wagon wheel damage—flat.

Wheel flats also occur from wheel slippage, wheel jamming, or braking equipment failures. Flats occur much more often in winter than in summer. The main reasons for the formation of the wheel flat are shown in Figure 4.

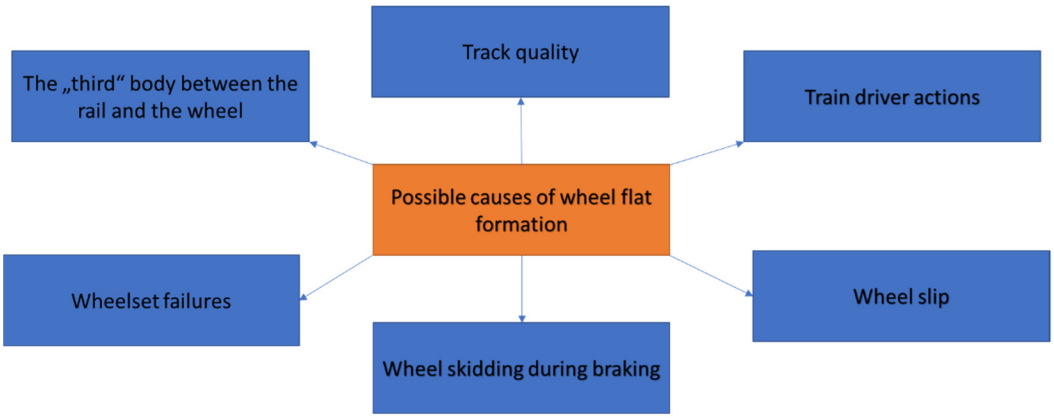

Figure 4. Main reasons of wheel flat formation.

Dynamic measurement methods include the vibration acceleration method, machine vision method, and YOLO deep learning network methods for wheel-rolling surface damage discovery. The operation of automatic crack detection system implemented based on YOLOv2 target detection, which improves the detection accuracy, is analyzed in the study [34]. Chinese researchers developed [35] a YOLOv3-based railway track line detection method that improved detection accuracy and speed. Furthermore, it preferred to incorporate lasers with images and, therefore, resulted in an structured light vision sensor (SLVS) sensor for assessing localized faults on wheel, such as a crack or wheel flat.

Various diagnostic systems can determine the magnitude of the damage based on the impact force. There are a lot of methods in the scientific literature to determine the correlation between these values [12] and the principles by which these systems operate [36]. On the other hand, rolling-stock wheelsets oscillate when rolling on a rail track [37]

(see Figure 5), so the wheel–rail contact points are not always on the same circle of the wheel rolling surface [38].

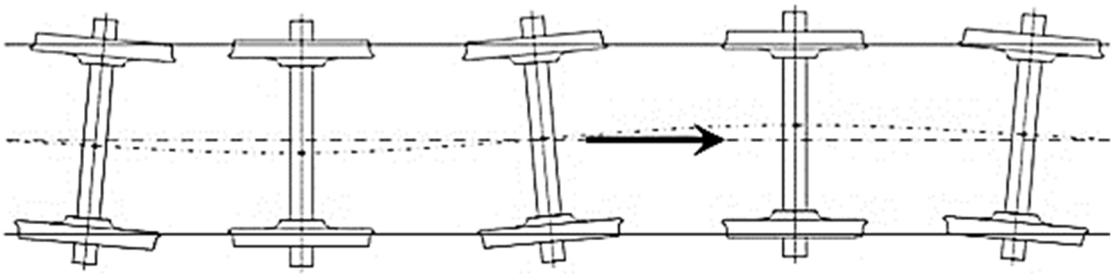

Figure 5. Wheelset oscillation of on the track.

Different detection methods have their advantages and disadvantages. Some methods have low detection accuracy or high actual operating costs. Therefore, the search for a more precise method has become a relevant issue.

Due to oscillation processes, the damaged wheel impacts on the rail at different surface points at each time, and the impact force varies. In operation, it is impossible to determine which of the measured values of the impact force is the most accurate (actual). It needs to be clarified on which basis the diagnostic equipment should estimate the magnitude of the damage.

3. Research Methodology

At first, the study compares the results of measuring vertical forces by different systems. In the same graph, the force values obtained from the ATLAS LG system are plotted on one axis and the special designed measurement system IC VEIP on the other. The view of both used measurement systems is presented in Figure 6.

(**a**) (**b**)

Figure 6. Used measurement systems: (**a**) regular system ATLAS-LG; (**b**) specially designed system IC VEIP.

The measuring range consists of 14 sleeper reaction measuring points (R-points) and 12 axle load measuring points (T-points). The last T-point is used for identifying wheelsets. Vertical impact on rail and static axle load of wheels is measured by strain gauges mounted on the rail neck. The main particularities are: ATLAS-LG system measures directly the vertical force, while the IC-VEIP system measures the rail acceleration and then converts it into a force value.

The best result is when the readings of both systems coincide. This result would indicate that both systems are equally suitable for studies on the influence of wagon wheelset damage on the nature of vertical forces. If all values are in a straight line and the line is formed at a different angle with the axes, it would mean that there is a systematic error in at least one of the systems. If the values are not in a straight line (scattered in the

plane), then the measurement results are not related to different systems, and at least one system is unsuitable for the test. Another important issue is estimating the scattering field for the measured force values. The box and whisker principle is used in the study [39].

The box and whisker graph is convenient in that it shows where the median of the values is (see Figure 7). It also shows where the 50% of values closest to the median (upper quartile and lower quartile) are distributed, the range of the remaining values (upper extreme and lower extreme). In addition, this type of graph can show individual values that stand out from the whole (outlier). A median value is used, taking into account the specific algorithm of the box and whisker method. This type of graph is very suitable for evaluating the repeatability of experimental results. Understandably, the better the repeatability of the results, the smaller the scatter fields of the values. An example of the application of the box and whisker principle is shown in Figure 7.

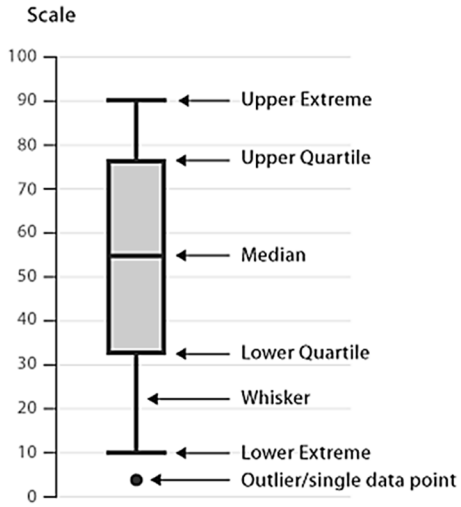

Figure 7. Example of application of box and whisker principle.

In the middle of the diagram in Figure 7, there are two middle quartiles. They are the limits between which half of all measurement values are distributed (twice 25%—two quartiles). In the middle of these quartiles, there is a median–mean value. The remaining values are outside these limits, and the authors did not analyze these values.

The ratio of the total width of the two middle quartiles to the median in estimating the wagon wheel damage magnitudes is calculated as:

$$Q_M = \frac{Q_U - Q_L}{M} \rightarrow min \quad (1)$$

where Q_u—upper quartile; Q_L—lower quartile; M—median (Figure 6).

For simplicity, this indicator name is sometimes abbreviated to indicator Q_M. This methodology estimates the ratio of the wheel-to-rail scattering field to the median Q_M. Such an indicator is important in proving that the size of the scatter field of impact values is less significant at high force values. Therefore, the lower value of the indicator Q_M shows better repeatability of the measured vertical force. The value of Q_M is calculated under different operating conditions of the rolling stock (in this case—different speeds). Comparing the Q_M values in different cases determined the states that are best suited to relate the magnitude of the damage to its vertical impact on the rail.

4. Measurement of Vertical Forces Caused by Wheel Damages

The operation in summer conditions of the standard ATLAS-LG and the special designed IC VEIP measurement systems was compared. The measurement results of the standard system, ATLAS-LG, were compared too. When the wheels of a rolling vehicle

act on the rails, each system captures the vertical force's basic (mean) values and the maximal values. Graphical interpretations of test results are provided in Figures 8 and 9.

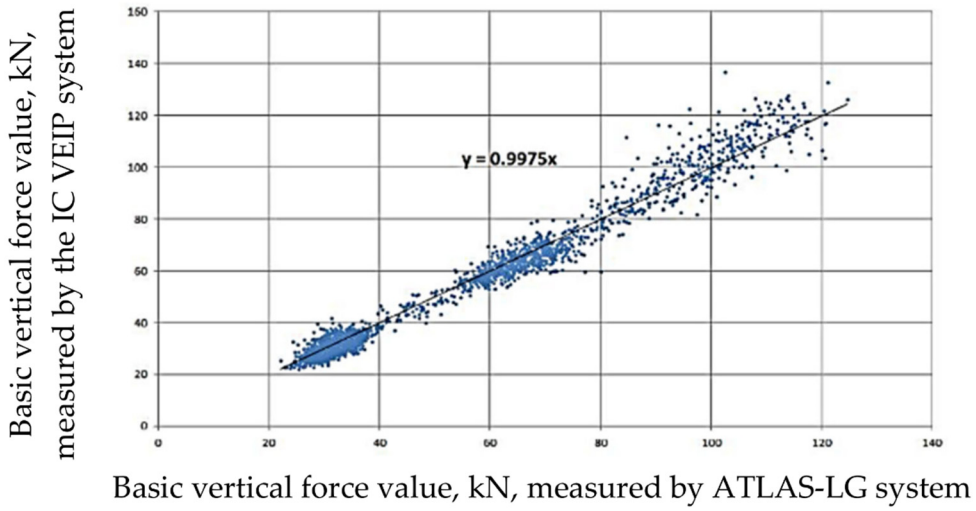

Figure 8. Correlation of measured values of basic vertical forces according to measurement systems.

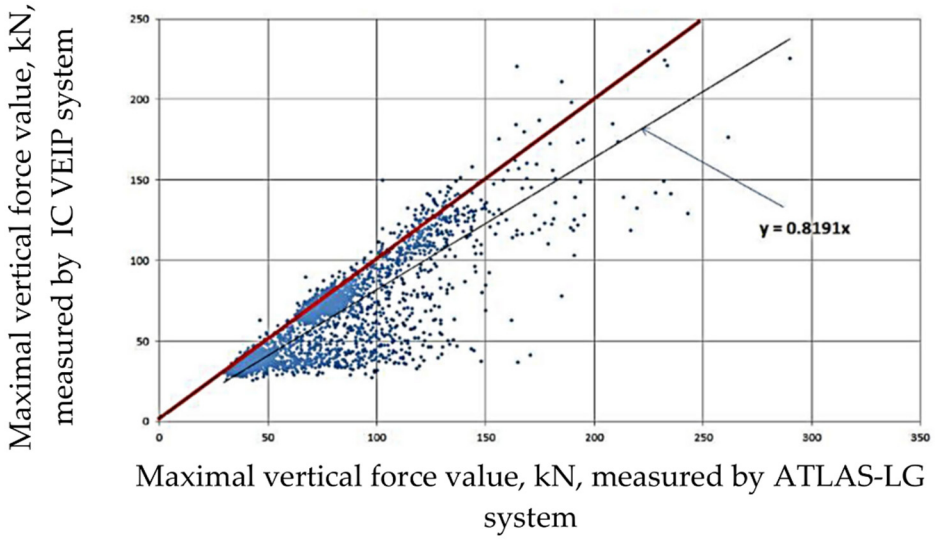

Figure 9. Correlation of measured values of maximal vertical forces according to measurement systems.

Since the curves of Figure 8 show the base forces (mean forces around the entire circumference of the wheel), their values are lower than the maximal forces shown in Figure 9. An analysis of the data in Figure 8 shows that the points corresponding to the mean force values are arranged along the hemisphere of the coordinate axes. That means that the measurement results of both systems are very similar, and the systems are equally suitable for research. Figure 8 shows a slightly wider scatter of the maximal load values while the trend remains the same. The field of values is arranged in a hemisphere of coordinates. The scatter of the values needs to be assessed using the appropriate methods presented below. Finally, the measurement results of the considered systems are equivalent, so the type of wayside measurement system does not have a significant impact on the repeatability of the measurement of vertical forces.

5. Distribution of Values of Wheel Vertical Forces

The authors propose to use the ratio of the total width of the two middle quartiles of the scattering field of the vertical force values to the median (indicator Q_M, Formula (1)) to examine the impact of the wheel-rolling surface damage on the measurement repeatability of the vertical forces. Two wheel-rolling surface damage types were selected for this study. For each damage type (shape), the vertical forces caused by the wheel damage were measured in four dimensions. Four data sets were obtained: mean values of vertical forces of unloaded wagon and of loaded; values of maximal vertical forces of unloaded wagon and of loaded wagon.

First, the test was performed with the damaged left wheel of the first wheelset. The wheel has two 20 × 10 × 4 mm and 15 × 40 × 3 mm cracks. Wheel damages provided in Figure 10.

Figure 10. Two cracks in the wagon's first wheelset wheel.

Box and whisker values of the maximal vertical forces of loaded goods wagon are shown Figure 11.

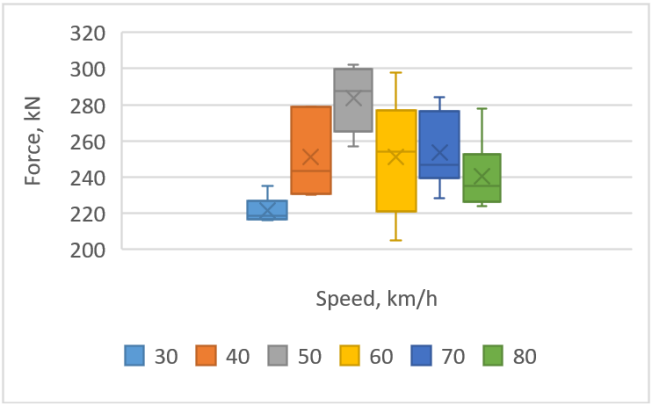

Figure 11. Maximal force values of loaded wagon.

The values of the indicator Q_M, calculated by the Formula (1) of maximal vertical forces of the loaded wagon are provided in Figure 12.

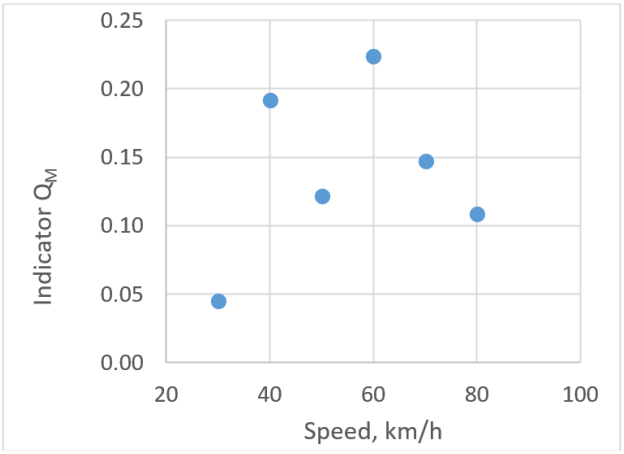

Figure 12. Values of Q_M, considering the maximal forces of loaded wagon.

The data in Figure 12 reveal that the influence of wagon wheel damage on the measurement of repeatability vertical forces is the highest at 30 km/h—lowest Q_M value, and the highest value is at a speed of 60 km/h. When wagon running speed increases, this impact on measurement repeatability decreases. It is inappropriate to perform tests at a speed of fewer than 30 km/h because, in this case, the amplitude of the carriage's oscillations may be lower than when driving at higher speeds, which would distort the adequacy of the results (equipment may not capture all damage). Since the tests are carried out on freight wagons, it is not appropriate to conduct them at speeds higher than 80 km/h. More test results were analyzed to better examine the dependences of wheel damage nature on repeatability. The values of the maximal vertical forces are given in the form of a box and whisker graph in Figure 13 when the goods wagon is unloaded.

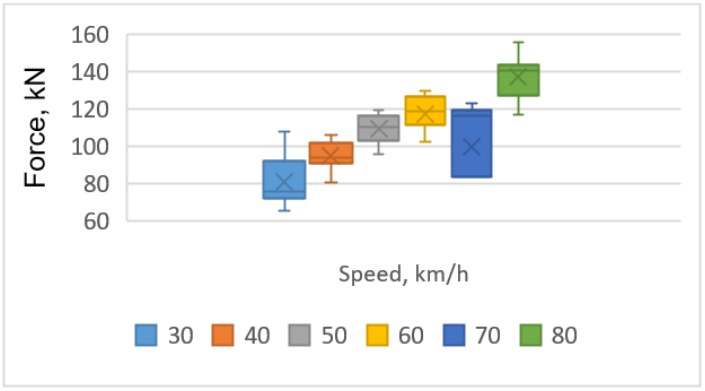

Figure 13. Values of maximal forces of unloaded goods wagon.

The chart of Figure 13 shows that the maximal scatter of the force values is at a speed level of 70 km/h. The values of Q_M, calculated according to Formula (1) for the maximal forces when the goods wagon is unloaded, are given in Figure 14.

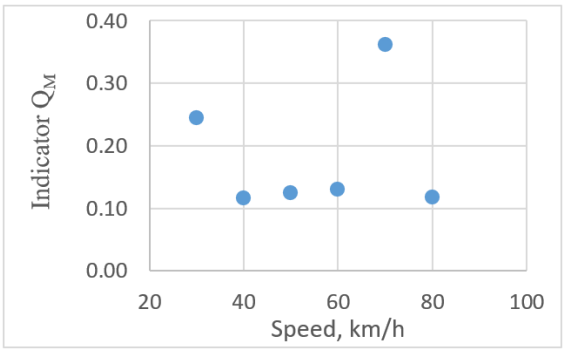

Figure 14. Values of Q_M, considering the maximal forces when unloaded goods wagon.

The data in Figure 14 reveal that the impact of wheel damage on the repeatability of measurement of vertical forces is the best (the lowest values of the indicator Q_M) at a speed of 40–60 km/h. More test results were analyzed to examine these dependencies better. The values of the mean vertical forces of loaded goods wagon are given in Figure 15.

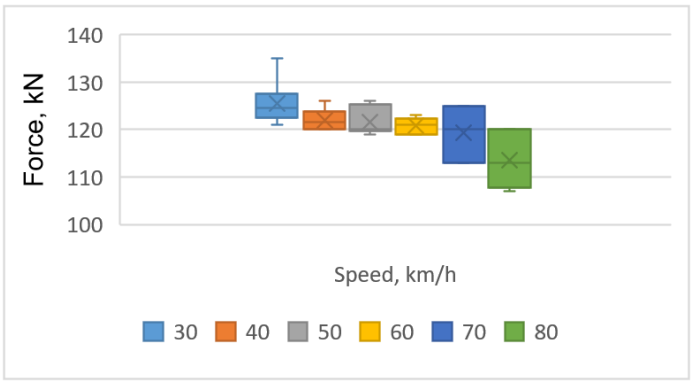

Figure 15. Mean values of vertical force when the wagon is loaded.

The chart of Figure 15 clearly disclose that as the wagon speed increases, the dispersion of the mean vertical forces increases. The values of Q_M with the loaded wagon are shown in Figure 16.

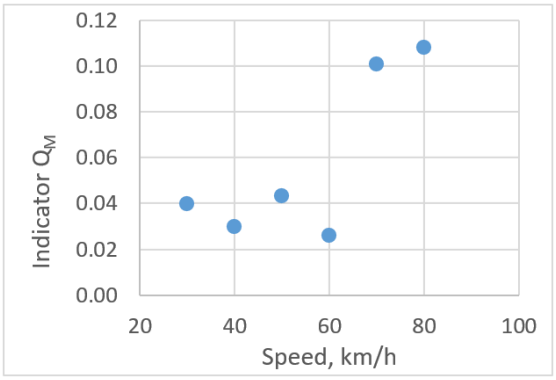

Figure 16. Values of the indicator Q_M, according to the mean vertical forces of loaded wagon.

The data in Figure 16 disclose that the impact of wheel damage on measurement repeatability of vertical forces is best at speeds of 40 and 60 km/h. No clear law is seen here. More test results were analyzed to examine the correlations with measurement repeatability better. The values of the mean forces of unloaded wagon are given in Figure 17.

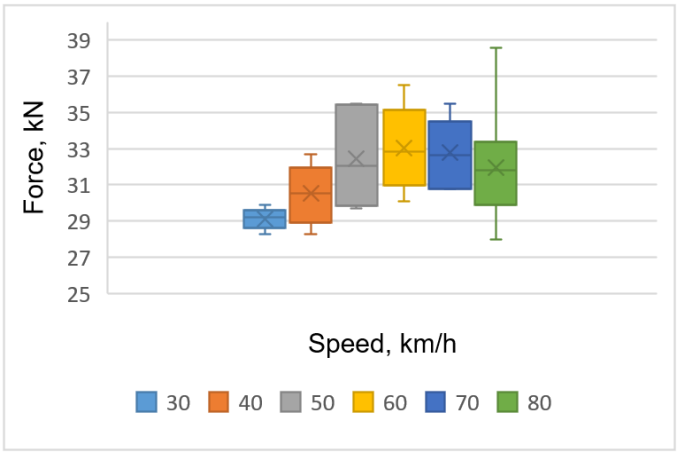

Figure 17. Vertical force mean values of unloaded wagon.

The chart of Figure 17 shows that the force dissipation is lowest at a speed of 30 km/h. The values of Q_M when the wagon is unloaded are given in Figure 18.

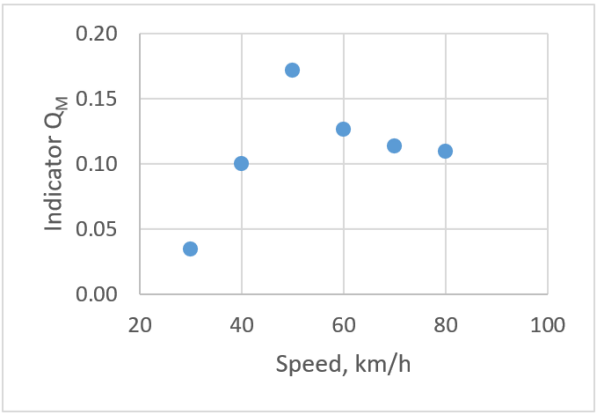

Figure 18. Values of Q_M considering to the mean vertical forces of unloaded goods wagon.

The data of Figure 18 show that the impact of wheel damage nature on the measurement repeatability of the vertical forces is best at a speed of 30 km/h.

For the second iteration of wheel damage testing, the damaged fourth wheel set's (in running direction) left wheel of the first wagon was selected: 87 × 30 × 2.0 mm flat and 30 × 40 × 2 mm cracks. Photos of wheel damage are provided in Figure 19.

Figure 19. Wheel damage—flat and cracks.

Examples of the distribution of vertical forces caused by wheel damage (flat and cracks) in rail cross-sections are provided in the literature [12].

Vertical force maximal values of loaded wagon are given in Figure 20.

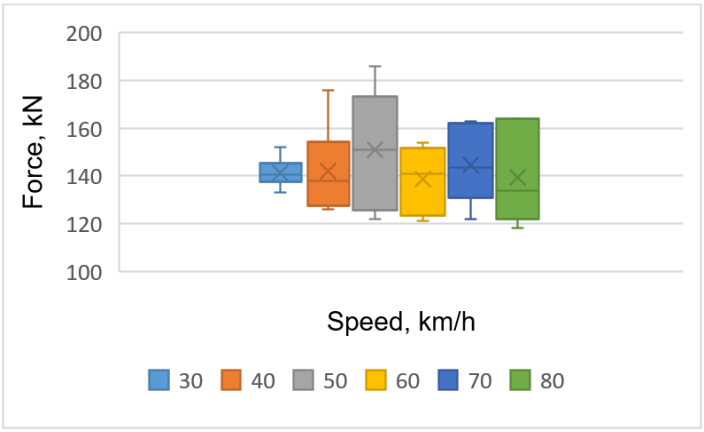

Figure 20. Maximal force values of loaded wagon (the second iteration).

The chart of Figure 20 shows that the scatter of the maximal vertical force values are lowest at the speed 30 km/h. The values of Q_M for the maximal vertical forces of loaded wagon are shown in Figure 20.

The data of Figure 21 reveal that the wagon wheel damage impact on measurement repeatability of vertical forces is best at a speed of 30 km/h. The values of the maximal forces of unloaded wagon are given in Figure 22.

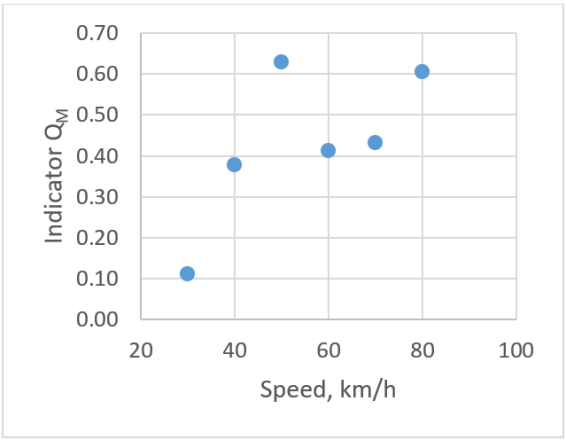

Figure 21. Values Q_M considering the loaded wagon maximal vertical forces.

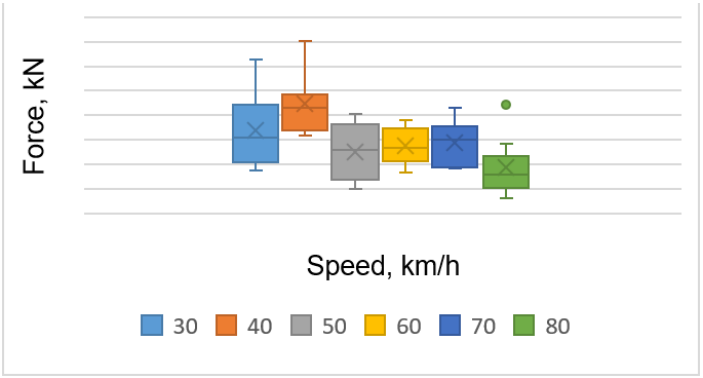

Figure 22. Maximal force values of unloaded goods wagon.

The data of Figure 23 show that the scattering field of the maximal vertical forces is the lowest at speed of 40 km/h and 60 km/h. The values of Q_M for the maximal vertical forces are given in Figure 22.

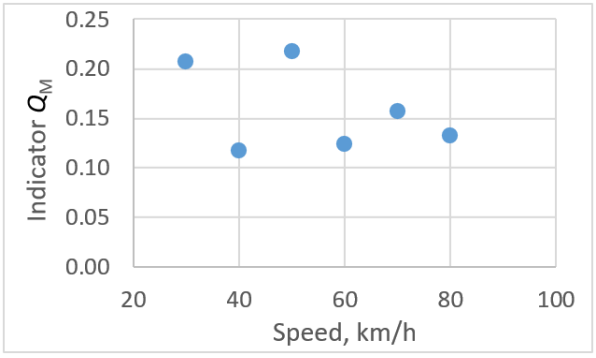

Figure 23. Values of Q_M considering to the maximal vertical forces of unloaded goods wagon.

The data of Figure 23 show that the wheel damage impact on measurement repeatability of vertical forces is best at speed of 40 km/h and 60 km/h. However, no clear pattern is seen here. In the case of the goods wagon being loaded, the vertical force mean values are given in Figure 24.

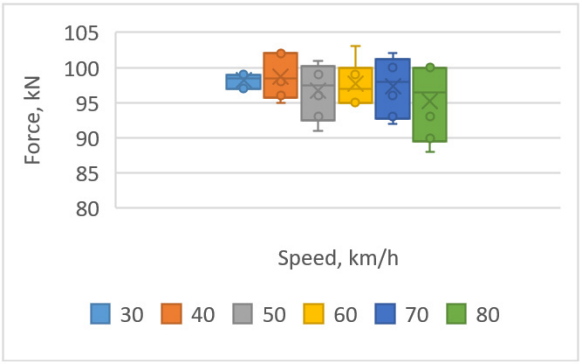

Figure 24. Vertical force mean values of loaded goods wagon.

The chart of Figure 24 shows that the dissipation of the mean forces is lowest when the wagon is at speed 30 km/h. The indicator Q_M values of loaded wagon are presented in Figure 25.

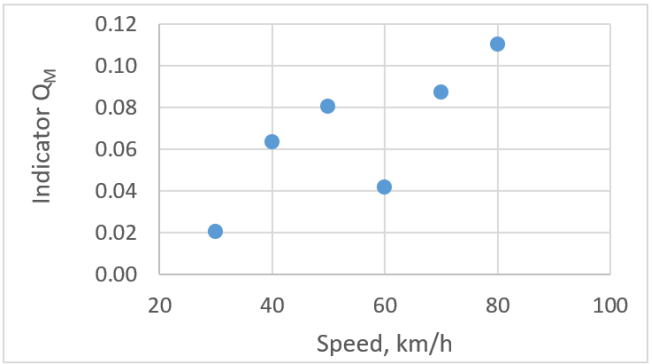

Figure 25. Values of Q_M considering the mean vertical forces of loaded goods wagon.

The data of Figure 25 show that the impact of wheel damage on measurement repeatability of vertical forces is best at a speed of 30 km/h. The mean values of the vertical forces of unloaded wagon are given in Figure 26.

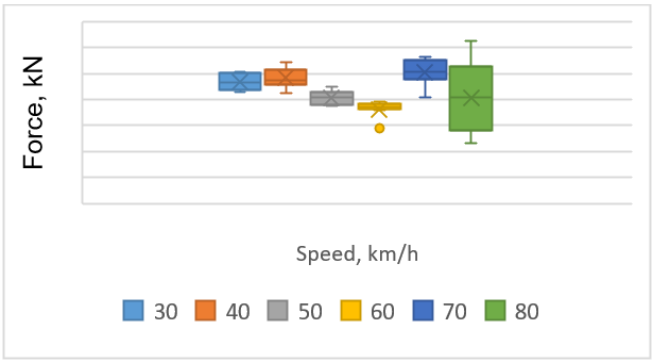

Figure 26. Vertical force mean values of unloaded goods wagon.

The chart of Figure 26 shows that the force dissipation field is the most significant at the speed of 80 km/h. The values of the indicator Q_M unloaded wagon are given in Figure 27.

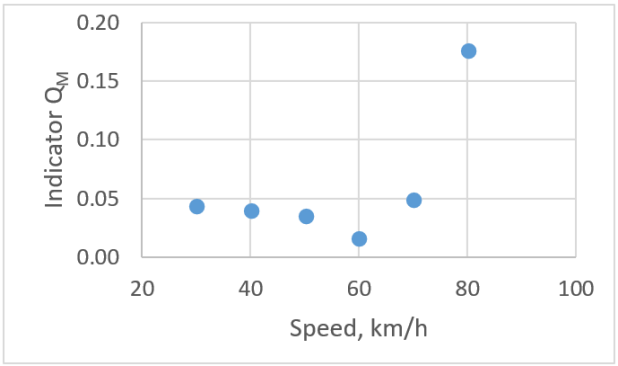

Figure 27. Values of Q_M considering the unloaded wagon mean vertical forces.

The data of Figure 27 show that the impact of wheel damage on measurement repeatability of vertical forces is best at a speed from 30 km/h to 60 km/h.

Summarized Q_M values are compiled based on the performed research. The final gained results are presented in Table 1.

Table 1. Summarized Q_M values.

Speed, km/h	The First Iteration of Force Testing				The Second Iteration of Force Testing			
	Max Forces		Mean Forces		Max Forces		Mean Forces	
	Loaded Wagon	Unloaded Wagon	Loaded Wagon	Unloaded Wagon	Loaded Wagon	Unloaded Wagon	Loaded Wagon	Unloaded Wagon
30	0.045	0.244	0.040	0.034	0.110	0.207	0.021	0.043
40	0.192	0.166	0.030	0.100	0.376	0.117	0.063	0.040
50	0.122	0.124	0.043	0.172	0.629	0.217	0.080	0.035
60	0.224	00.13	0.026	0.126	0.411	0.124	0.041	0.016
70	0.147	0.362	0.101	0.114	0.432	0.156	0.087	0.048
80	0.109	0.118	0.108	0.110	0.606	0.132	0.110	0.176

The arithmetic mean of the values is calculated for each row of Table 1 (running speed from 30 km/h to 80 km/h). Normalized values of this mean for appropriate speed are shown in Figure 28.

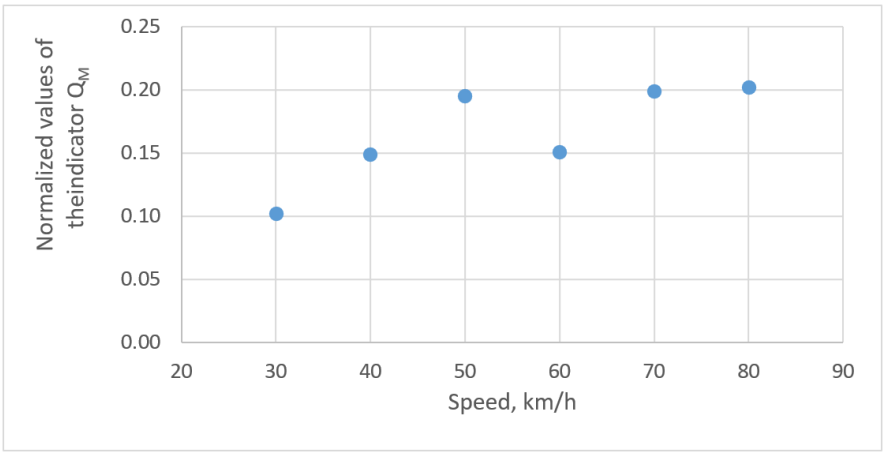

Figure 28. Normalized Q_M values according to the running speed.

The indicator Q_M is needed to assess the wheel damage influence on the repeatability of vertical force measurement values (Formula 1). A lower Q_M value means better measurement repeatability. Summarizing the results, the Q_M values are presented (Figure 28) in normalized form. It can be seen that decrease in running speed from 80 km/h to 50–60 km/h does not improve the correlation between the wheel damage and the vertical forces. To improve this correlation, reducing the speed to 30–40 km/h is needed.

6. Conclusions

Rolling stock wheelsets oscillate on the rail track, so the wheel–rail contact points are never on the same circle of the wheel rolling (contacting) surface. As a result of these processes, the wheel damage contacts the rail at different surface points at each moment, and the vertical impact force changes. During rolling-stock operation, it is impossible to determine which of the measured values of the impact force is the most accurate. The scattering field of the values is obtained during the measurements, and a methodology is required to process it. The investigation reveals that the box and whisker method is well-suited for analysing the scattering field of force measurement results.

The ratio of the total width of the two middle quartiles and the median is proven as the suitable indicator for assessing the effect of the car wheel clearance on the repeatability of vertical force measurements.

The authors reveal that of all the various factors that affect the repeatability of the measurement of wheel vertical force, speed is the only factor that has an obvious correlation. For other factors (e.g., type of measuring system, nature of wheel damage), no clear correlation is observed during the study.

The other disclosed aspect is that decreasing the running speed from 80 km/h to 50–60 km/h does not strengthen the correlation between the wheel damage nature and the repeatability of vertical force measurement. Greater reducing levels of train speed were applied to improve the quality of wagon wheel damage nature impact identification. Reduction in the train speed from 80 km/h to 30–40 km/h reduces the value of the indicator Q_M proposed by the authors by 1.5–2 times.

When operating the rolling stock and knowing the conditions under which the values of Q_M are the lowest, the repeatability of measurement of wheel/rail vertical forces is the highest.

In the future, the authors plan to study the repeatability of measurement results of systems operating on other principles. Furthermore, a limitation of this research is the incompatibility of the measuring systems ATLAS-LG and IC VEIP with other diagnostic systems used in railways. This devise incompatibility causes the low reproducibility of the results of the present study.

Author Contributions: Methodology, conceptualization and writing, G.V.; supervision, G.B.; investigation and formal analysis, S.S. All authors have read and agreed to the published version of the manuscript.

Funding: This research received no external funding.

Institutional Review Board Statement: Not applicable.

Informed Consent Statement: Not applicable.

Data Availability Statement: For commercial reasons, more detailed research data is not disclosed.

Conflicts of Interest: The authors declare no conflict of interest.

References

1. Bureika, G.; Vaičiūnas, G.; Shi, D.; Zanuy, A.C. Influence of Track Geometry Condition Monitoring on Railway Infrastructure Maintenance Processing. *Transp. Probl.* **2022**, *17*, 211–220. https://doi.org/10.20858/TP.2022.17.4.18.
2. Weston, P.F.; Ling, C.S.; Roberts, C.; Goodman, C.J.; Li, P.; Goodall, R.M. Monitoring Vertical Track Irregularity from In-Service Railway Vehicles. *Proc. Inst. Mech. Eng. Part F J. Rail Rapid Transit* **2016**, *221*, 75–88. https://doi.org/10.1243/0954409JRRT65.
3. Ramalho, A. Wear Modelling in Rail–Wheel Contact. *Wear* **2015**, *330–331*, 524–532. https://doi.org/10.1016/J.WEAR.2015.01.067.
4. Meymand, S.Z.; Keylin, A.; Ahmadian, M. A Survey of Wheel–Rail Contact Models for Rail Vehicles. *Veh. Syst. Dyn.* **2016**, *54*, 386–428. https://doi.org/10.1080/00423114.2015.1137956.
5. Aalami, M.R.; Anari, A.; Shafighfard, T.; Talatahari, S. A Robust Finite Element Analysis of the Rail-Wheel Rolling Contact. *Adv. Mech. Eng.* **2013**, *5*, 272350. https://doi.org/10.1155/2013/272350.
6. Thakkar, N.A.; Steel, J.A.; Reuben, R.L. Rail–Wheel Interaction Monitoring Using Acoustic Emission: A Laboratory Study of Normal Rolling Signals with Natural Rail Defects. *Mech. Syst. Signal Process.* **2010**, *24*, 256–266. https://doi.org/10.1016/J.YMSSP.2009.06.007.
7. Roy, T.; Lai, Q.; Abrahams, R.; Mutton, P.; Paradowska, A.; Soodi, M.; Yan, W. Effect of Deposition Material and Heat Treatment on Wear and Rolling Contact Fatigue of Laser Cladded Rails. *Wear* **2018**, *412–413*, 69–81. https://doi.org/10.1016/J.WEAR.2018.07.001.
8. Datsyshyn, O.P.; Panasyuk, V.V.; Glazov, A.Y. Modeling of Fatigue Contact Damages Formation in Rolling Bodies and Assessment of Their Lifetime. *Wear* **2011**, *271*, 186–194. https://doi.org/10.1016/J.WEAR.2010.10.023.
9. Seo, J.; Kwon, S.; Lee, D. Effects of Surface Defects on Rolling Contact Fatigue of Rail. *Procedia Eng.* **2011**, *10*, 1274–1278. https://doi.org/10.1016/J.PROENG.2011.04.212.
10. Burdzik, R.; Konieczny, Ł.; Deuszkiewicz, P.; Vaskova, I. Application of Time-Frequency Method for Research on Influence of Locomotive Wheel Slip on Vibration. *J. Vibroeng.* **2018**, *20*, 2998–3008. https://doi.org/10.21595/JVE.2018.20450.
11. Dižo, J.; Blatnický, M.; Gerlici, J.; Leitner, B.; Melnik, R.; Semenov, S.; Mikhailov, E.; Kostrzewski, M. Evaluation of Ride Comfort in a Railway Passenger Car Depending on a Change of Suspension Parameters. *Sensors* **2021**, *21*, 8138. https://doi.org/10.3390/S21238138.
12. Bureika, G.; Levinzon, M.; Dailydka, S.; Steisunas, S.; Zygiene, R. Evaluation Criteria of Wheel/Rail Interaction Measurement Results by Trackside Control Equipment. *Int. J. Heavy Veh. Syst.* **2019**, *26*, 747–764. https://doi.org/10.1504/IJHVS.2019.102682.
13. Celiński, I.; Burdzik, R.; Młyńczak, J.; Kłaczyński, M. Research on the Applicability of Vibration Signals for Real-Time Train and Track Condition Monitoring. *Sensors* **2022**, *22*, 2368. https://doi.org/10.3390/S22062368.
14. Burdzik, R.; Słowiński, P.; Juzek, M.; Nowak, B.; Rozmus, J. Dependence of Damage to the Running Surface of the Railway Rail on the Vibroacoustic Signal of a Passing Passenger Train. *Vibroeng. Procedia* **2018**, *19*, 226–229. https://doi.org/10.21595/VP.2018.20232.
15. Wallentin, M.; Bjarnehed, H.L.; Lundén, R. Cracks around Railway Wheel Flats Exposed to Rolling Contact Loads and Residual Stresses. *Wear* **2005**, *258*, 1319–1329. https://doi.org/10.1016/J.WEAR.2004.03.041.
16. Popp, K.; Kruse, H.; Kaiser, I. Vehicle-Track Dynamics in the Mid-Frequency Range. *Veh. Syst. Dyn.* **1999**, *31*, 423–464. https://doi.org/10.1076/VESD.31.5.423.8363.
17. Steinfeld, A.; Fong, T.; Kaber, D.; Lewis, M.; Scholtz, J.; Schultz, A.; Goodrich, M. Common Metrics for Human-Robot Interaction. In Proceedings of the HRI 2006: Proceedings of the 2006 ACM Conference on Human-Robot Interaction, Salt Lake City, UT, USA, 2–3 March, 2006; pp. 33–40. https://doi.org/10.1145/1121241.1121249.
18. Ma, L.; Shi, L.B.; Guo, J.; Liu, Q.Y.; Wang, W.J. On the Wear and Damage Characteristics of Rail Material under Low Temperature Environment Condition. *Wear* **2018**, *394–395*, 149–158. https://doi.org/10.1016/J.WEAR.2017.10.011.
19. Fang, Z.; Lou, L.; Tang, K.; Wang, W.; Chen, B.; Wang, Y.; Zheng, Y. A CMOS-Integrated Radar-Assisted Cognitive Sensing Platform for Seamless Human-Robot Interactions. In Proceedings of the IEEE International Symposium on Circuits and Systems, Daegu, Korea, 22–28 May 2021. https://doi.org/10.1109/ISCAS51556.2021.9401535.
20. Wang, W.J.; Liu, T.F.; Wang, H.Y.; Liu, Q.Y.; Zhu, M.H.; Jin, X.S. Influence of Friction Modifiers on Improving Adhesion and Surface Damage of Wheel/Rail under Low Adhesion Conditions. *Tribol. Int.* **2014**, *75*, 16–23. https://doi.org/10.1016/J.TRIBOINT.2014.03.008.

21. Pieringer, A.; Kropp, W.; Nielsen, J.C.O. The Influence of Contact Modelling on Simulated Wheel/Rail Interaction Due to Wheel Flats. *Wear* **2014**, *314*, 273–281. https://doi.org/10.1016/J.WEAR.2013.12.005.
22. Wang, W.J.; Guo, H.M.; Du, X.; Guo, J.; Liu, Q.Y.; Zhu, M.H. Investigation on the Damage Mechanism and Prevention of Heavy-Haul Railway Rail. *Eng. Fail. Anal.* **2013**, *35*, 206–218. https://doi.org/10.1016/J.ENGFAILANAL.2013.01.033.
23. Konowrocki, R.; Chojnacki, A. Analysis of Rail Vehicles' Operational Reliability in the Aspect of Safety against Derailment Based on Various Methods of Determining the Assessment Criterion. *Eksploat. I Niezawodn.* **2020**, *22*, 73–85. https://doi.org/10.17531/EIN.2020.1.9.
24. Huang, Y.B.; Shi, L.B.; Zhao, X.J.; Cai, Z.B.; Liu, Q.Y.; Wang, W.J. On the Formation and Damage Mechanism of Rolling Contact Fatigue Surface Cracks of Wheel/Rail under the Dry Condition. *Wear* **2018**, *400–401*, 62–73. https://doi.org/10.1016/J.WEAR.2017.12.020.
25. Regularities of Shaping of a Wheel Profile as a Result of Deterioration of the Rolling Surface in Exploitation-Transport Problems-Tom T. 3, z. 4 (2008)-BazTech-Yadda. Available online: https://yadda.icm.edu.pl/baztech/element/bwmeta1.element.baztech-article-BSL7-0032-0017 (accessed on 9 March 2022).
26. Shevtsov, I.Y.; Markine, V.L.; Esveld, C. Design of Railway Wheel Profile Taking into Account Rolling Contact Fatigue and Wear. *Wear* **2008**, *265*, 1273–1282. https://doi.org/10.1016/J.WEAR.2008.03.018.
27. Jin, X.; Xiao, X.; Wen, Z.; Guo, J.; Zhu, M. An Investigation into the Effect of Train Curving on Wear and Contact Stresses of Wheel and Rail. *Tribol. Int.* **2009**, *42*, 475–490. https://doi.org/10.1016/J.TRIBOINT.2008.08.004.
28. Polach, O. Wheel Profile Design for Target Conicity and Wide Tread Wear Spreading. *Wear* **2011**, *271*, 195–202. https://doi.org/10.1016/J.WEAR.2010.10.055.
29. Vaičiūnas, G.; Bureika, G.; Steišūnas, S. Research on Metal Fatigue of Rail Vehicle Wheel Considering the Wear Intensity of Rolling Surface. *Eksploat. I Niezawodn.* **2018**, *20*, 24–29. https://doi.org/10.17531/EIN.2018.1.4.
30. Turnia, J.; Sinclair, J.; Perez, J. A Review of Wheel Wear and Rolling Contact Fatigue. *J. Rail Rapid Transit* **2007**, *221*, 271–289. https://doi.org/10.1243/0954409JRRT72.
31. Bodini, I.; Petrogalli, C.; Faccoli, M.; Lancini, M.; Pasinetti, S.; Sansoni, G.; Docchio, F.; Mazzù, A. Evaluation of Wear in Rolling Contact Tests by Means of 2D Image Analysis. *Wear* **2018**, *400–401*, 156–168. https://doi.org/10.1016/J.WEAR.2017.12.023.
32. Tamada, R.; Shiraishi, M. Prediction of Uneven Tire Wear Using Wear Progress Simulation. *Tire Sci. Technol.* **2017**, *45*, 87–100. https://doi.org/10.2346/TIRE.17.450201.
33. Favorskaya, A.; Khokhlov, N. Modeling the Impact of Wheelsets with Flat Spots on a Railway Track. *Procedia Comput. Sci.* **2018**, *126*, 1100–1109. https://doi.org/10.1016/J.PROCS.2018.08.047.
34. Chen, Y.; Li, Y.; Niu, G.; Zuo, M. Offline and Online Measurement of the Geometries of Train Wheelsets: A Review. *IEEE Trans. Instrum. Meas.* **2022**, *71*, 3523915. https://doi.org/10.1109/TIM.2022.3205691.
35. Wei, X.; Wei, D.; Suo, D.; Jia, L.; Li, Y. Multi-Target Defect Identification for Railway Track Line Based on Image Processing and Improved YOLOv3 Model. *IEEE Access* **2020**, *8*, 61973–61988. https://doi.org/10.1109/ACCESS.2020.2984264.
36. Vaičiūnas, G.; Bureika, G.; Steišūnas, S. Rail Vehicle Axle-Box Bearing Damage Detection Considering the Intensity of Heating Alteration. *Eksploat. I Niezawodn.–Maint. Reliab.* **2020**, *22*, 724–729. https://doi.org/10.17531/EIN.2020.4.16.
37. Qu, S.; Wang, J.; Zhang, D.; Li, D.; Wei, L. Failure Analysis on Bogie Frame with Fatigue Cracks Caused by Hunting Instability. *Eng. Fail. Anal.* **2021**, *128*, 105584. https://doi.org/10.1016/J.ENGFAILANAL.2021.105584.
38. Matsumoto, A.; Sato, Y.; Ohno, H.; Tomeoka, M.; Matsumoto, K.; Ogino, T.; Tanimoto, M.; Oka, Y.; Okano, M. Improvement of Bogie Curving Performance by Using Friction Modifier to Rail/Wheel Interface: Verification by Full-Scale Rolling Stand Test. *Wear* **2005**, *258*, 1201–1208. https://doi.org/10.1016/J.WEAR.2004.03.063.
39. Larsen, R.D. Box-and-Whisker Plots. *J. Chem. Educ.* **1985**, *62*, 302–305. https://doi.org/10.1021/ED062P302.